Conformational Conversion and Local Packing of Cyclic Olefin Copolymers

Peter Po-Jen Chu* and Men-Hsung Cheng

Department of Chemistry, National Central University, Chung-Li, Taiwan, R.O.C.

Wu-Jang Huang and Feng-Chih Chang

Institute of Applied Chemistry, National Chiao-Tung University, Hsin-Chu, Taiwan, R.O.C.

Received March 21, 2000; Revised Manuscript Received May 31, 2000

ABSTRACT: Cyclic olefin copolymer (COC, poly(norbornene-*co*-ethylene)) catalyzed by *ansa*-ethylenebis-(indenyl)zirconium dichloride ($Et[Ind]_2ZrCl_2$)/methylaluminoxane (MAO) gives rise to phenomenal increase of T_g upon annealing. Unaveraged solid-state ^{13}C NMR resonance of the CH carbons in the norbornene (53 and 49 ppm) evidenced the conformation conversion from T[X]T and G[X]G to more stable T[X]G conformers (where [X] = [T] or [G] represent the norbornene chain conformation). As the persistent length increases with the conversion, local packing of the rigid chain subsequently occurs. Synchrotron source X-ray diffraction provides clear evidence of the averaged interchain contraction from 12.0 to 8.5 Å and a tighter distribution in the spacing after annealing. In the preannealed state, $T_{1\rho}{}^H$ relaxation time revealed both mobile (where conformer converts) and rigid components (where conformation is frozen), which coalesce into a further rigid component after extended annealing. The mechanisms governing the packing in amorphous COC are likely by the random chain diffusion and not from cooperative motion as described by the bundle-packing model.

Introduction

Cyclic olefin copolymers (COC) synthesis and characterization have been the subject of many researches. The copolymers receive new thrust with recent developments of metallocene technologies.[1−9] Prior studies have shown that T_g up to 260 °C and a melting temperature (T_m) near 400 °C can be reached for polynorborene homopolymer.[6−8] Fink et al. reported that COC with the norbornene (NB) microblock varying from isolated, alternating NB and longer NB block structures can be produced by tailoring metallocene and half-sandwich catalysts.[9] In this study, we present the structural characterization of a series of COC's synthesized with *ansa*-ethylenebis(indenyl)zirconium dichloride (*rac*-$Et[Ind]_2ZrCl_2$). Because of the rigidity of the NB unit, the conformation conversion is highly restricted, and the conformers were "frozen" after polymerization. Previous ^{13}C solid-state NMR studies had identified unaveraged chain conformations in the condensed phase.[10] Heating provided the energy to convert to the most energetically favored conformer which leads to an increase of the persistent length and a more rigid chain segment. Amorphous polymers containing rigid monomer unit, such as polycarbonate (PC),[11] poly(phenylene sulfide) (PPS),[12] poly(ethyl ether ketone) (PEEK),[13] and polyimide (PI),[14] are reported to exhibit ordered local packing, likely by the process described above. However, the true mechanism remains ambiguous. At least two models have been proposed to describe the packing process. The random packing model of Suter et al.[15] considered minimization of entropy between rigid segments of neighboring chains, and the bundle-packing model by Whitney and Yaris involves pairwise chain arrangement with specific proximity to create local order.[16] In the case of bisphenol A polycarbonate, interchain internuclear distances measured by solid-state NMR have been interpreted in terms of the bundle model in the glassy state.[17] For COC, in which the rigid NB block served as the rigid linker and the adjacent ethylene unit the flexible extender, the polymer is also capable of rearranging into higher ordered local packing. The present work focuses on the process of such packing, which would be directly responsible for the phenomenal increase of glass temperature in COC upon annealing. Possible mechanisms and structural factors influencing the condensation will be discussed.

* Corresponding author. E-mail: pjchu@rs970.ncu.edu.tw.

Experimental Section

COC from norbornene and ethylene was synthesized according to the procedure described previously using *ansa*-metallocene catalyst $Et(Indenyl)_2ZrCl_2$/MAO.[2−8,18] Cocatalyst/catalyst mole ratio of 3000−7000 were employed. The polymerization temperature was maintained at ∼70 °C with constant ethylene pressure of 19−21 psi (ca. 1.5 bar). The ethylene pressure is much lower and the reaction temperature higher than those used by Ruchatz et al. where ethylene pressure is 1−10 bar and the reaction temperature is 30−40 °C.[19] Microstructures of these copolymers were characterized by solution ^{13}C NMR (ν_C = 50 MHz) using 5 wt % solution in trichlorobenzene (TCB) at elevated temperature (120 °C). The alternating, isolated, and block norbornene contents are determined following the prescribed characterization procedures with ^{13}C NMR.[19−24] Glass temperatures were determinate by DSC (Perkin-Elmer DSC-7) with a heating rates of 10 °C/min. The scanning temperature was limited from 30 to 220 or 300 °C to avoid sample degradation. Sample annealing was conducted on a vacuum oven at 30 °C above the initial T_g for controlled duration. Solid-state ^{13}C NMR (ν_C = 100.24 MHz) spectra were recorded with strong proton decoupling (H_1 = 85 kHz) with a spinning rate close to 8 kHz. Proton spin−lattice relaxation time in the rotating frame, $T_{1\rho}{}^H$, is measured indirectly from carbon signals with strong spin-lock field.

X-ray diffraction was conducted using a synchrotron source (Synchrotron Radiation Research Center, Hsin-Chu, Taiwan) on a Japan MacScience Co. (M18XHF-SRA) diffractometer with a scanning rate of 2°/min at room temperature.

10.1021/ma000494k CCC: $19.00
Published on Web 11/17/2000

Table 1. High-Resolution ^{13}C NMR Analysis Results of Cycle Olefin Copolymers (COC's)[a]

run	NB content (mol %)	NB sequence (mol %) block (−N−N− and higher)	alternating	isolated
1	100.0	100.0	0	0
3	58.36	40.16	51.85	7.99
4	47.63	50.21	40.55	9.25
5	43.51	17.33	66.60	16.07
6	24.88	21.02	51.04	27.98

[a] Polymerization conditions: ethylene pressure = 20 psi, 70°C; total volume = 60 mL; [Al]/[Zr] = 8000−4000; catalyst = 1−2 mg.

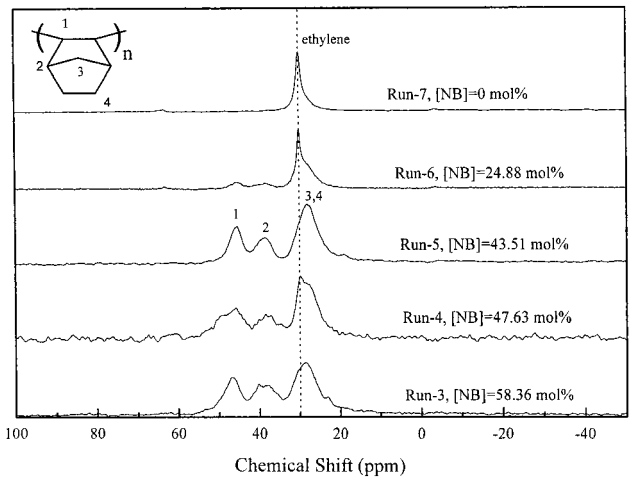

Figure 1. Solid-state NMR ^{13}C NMR cross-polarization with magic angle spinning (CP/MAS) spectra of run 3 to run 7.

Results and Discussion

The microstructure and the mole fraction of the three main NB microblock signatures (alternating, isolated, and block) for the COC studied are summarized in Table 1. Different norbornene feed ratio leads to copolymers with varying NB and ethylene segmental lengths. The higher reaction temperature used in this study raises the norbornene activity ratio, and the two-carbon bridge in the catalyst created an opening wide enough for more continuous norbornene (NB) units to be included. The COC produced here contains a higher amount of NB block (−N−N−N− and −N−N−) compared to other COC samples of the same NB content using different catalysts. [23−25]

Figure 1 displays normal solid-state ^{13}C NMR CP/MAS spectra of sample runs 3−7 (pure PE). The major peaks (labeled in the inset) correspond to the backbone carbon (CH, peak 1), bridgehead carbon, (CH, peak 2), and one- and two-atom bridged carbons (CH_2, peaks 3 and 4). Different NB microblock structure signals are not well resolved in solid since the strong dipolar−dipolar interaction and the inhomogeneous chemical shift distribution in the amorphous state smear the characteristics. The 30 ppm peak (methylene from PE) increases with increasing PE feed, but the line width becomes much broader compared with that of PE homopolymer. Peaks 1−4 are also broader, but the center has shifted to that for the block NB unit in solution. More severe overlapping is detected for peaks 3 and 4 in solid NMR, and additional downfield resonances, not identified in the solution phase, are found.

***T_g* Variation with Annealing**. As seen in Figure 2, substantial increases of T_g for all COC samples are observed with heat treatment at 30 °C above initial T_g,. Depending on the NB content (mole percent), the degree of changes in T_g before and after annealing occurs in the range of 15−116 °C (Table 2). In addition, the final T_g where equilibrium is reached increases with increasing NB. Interestingly, pure PNB shows an initial T_g of 135 °C which increases to 252 °C (the plateau value), with nearly 120 °C jump after annealing. This value is comparable with T_g of compression-molded COC products (∼250 °C) where [NB] content is 98 mol %.[7,10] For other COCs examined, T_g variation occurred on the order of 30−80 °C. The unusual T_g variation is indicative of the metastable state in the as-prepared glassy COC and PNB samples. Although other amorphous polymers containing rigid repeating unit have also displayed T_g variation on the order of ca. 5−8 °C after heat treatment, a substantial change as observed here is rather unusual.

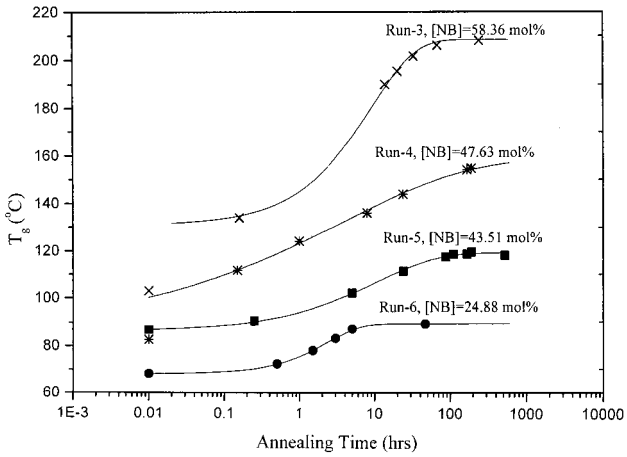

Figure 2. An apparent increase of T_g with annealing which plateaus for all COC sample after annealing for ∼200 h is observed.

Table 2. Characteristics of Cycle Olefin Copolymers Studied

run	NB content (mol %)	T_g (°C) as prepared	T_g (°C) after annealing[b]
1	100	136.2	216.9 (252*)
3	58.38	102.5	179.9
4	47.63	81.3	154.5
5	43.51	86.8	119.6
6	24.88	68.1	98.0
7[a]	0	<0	<0

[a] Pure PE. [b] Plateau value from the uppermost curve in Figure 2.

Conformation Conversion. For samples containing over 47.63 mol % norbornene content (runs 1, 3, and 4), a rapid T_g jump (over 32 °C) during initial annealing stage is apparent. (Figure 2 and Table 2). In those samples, solid-state ^{13}C NMR unravels systematic changes with heat treatment. Shown in Figure 3 are the ^{13}C spectrum of run 1 (PNB), run 4 ([NB] = 47.63 mol %), and run 6 ([NB] = 24.88 mol %). For both run 1 and run 4, partially resolved peaks are detected. The split feature is most prominent for the CH backbone carbons on NB monomer (peak 1) where two major groups of chemical shifts at 49 and 53 ppm are identified. Notice that the 53 ppm peak, which is absent in the solution spectrum, diminishes upon annealing. The different conformers established between consecutive single bonds in polymers comprise a variety of chemical shifts and broadens the individual resonance. Rapid

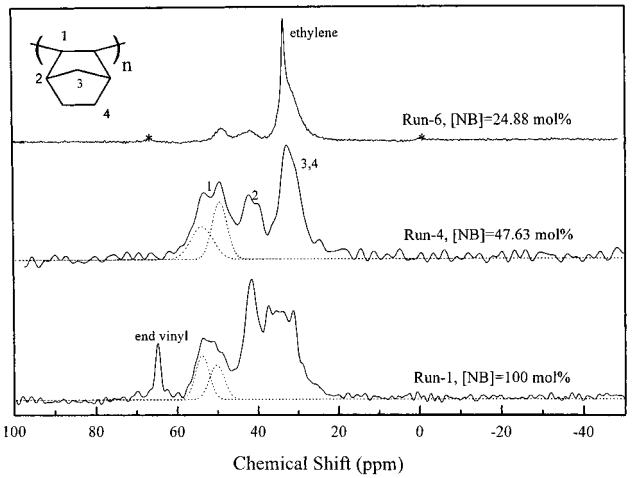

Figure 3. Solid-state ^{13}C NMR CP/MAS spectra for sample 1, run 4 and run 6. The assignment is labeled in the inset. The dashed curve represents the best fit with two Gaussian components.

interconversions between rotation isomers yield averaged absorption with breadth dependent upon the conversion rate. However, when the conversion is restricted, the conformers can be frozen at the local energy minimum. For example, the all-trans and $(ttgg)_n$ conformers in the crystalline syndiotactic polystyrene (identified by the resolved ^{13}C NMR separated ~1 ppm) [26] cannot be averaged or converted with extensive heat treatment, unless a small amount of solvent is present. Since COC is totally amorphous, the well-resolved peaks (spaced 2−4 ppm) shown in Figure 3 are intriguing as well as surprising. These peaks with ~4 ppm separation are not originated from difference in microstructures (such as tacticity and microblock) since they cannot be removed or created simply by heating under vacuum. The present result is, however, more akin to that of PET where the cis conformer is reduced during crystallization. Detailed characterization confirmed that conversion occurs in the interface between the amorphous and the crystalline domain.[27] For COC, however, this conversion occurs entirely in the amorphous domain.

The NB ring structure behaves as a double bond; the conformation in the NB ring is predetermined during polymerization. The conformation conversion is achieved by rotation of the adjacent single bond, with energy barrier higher than that of the linear chain. The situation becomes aggravated when several norbornene units join in a continuous block. Failure to sample rapidly all possible conformations results in incomplete averaging of conformations in the amorphous solid. As a result of the restriction for rotation, multiple absorptions, instead of a broad resonance, corresponding to the individual conformers are observed for each structurally distinctive carbon. Annealing at elevated temperature overcomes the energy barrier to convert to a most stable state. This process is reflected directly in the disappearance of the downfield (53 and 42 ppm) resonance in COC.

The question remains regarding the identities for these conformations. To simplify the following discussion, we resort to conventional nomenclature for trans and gauche conformations. Scheme 1 demonstrated that a gauch (G) form corresponds to both cis-exo and cis-endo conformations and a trans (T) form to the exo-endo conformation on the norbornene. For convenience, the norbornene confirmation is denoted with brackets.[28]

Scheme 1. Configuration of Norbornene Unit

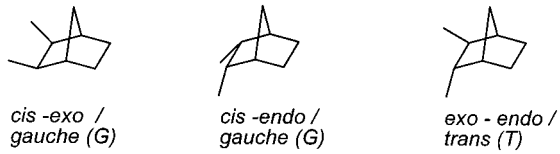

Scheme 2. Typical Configuration of Syndiotactic Polynorbornene

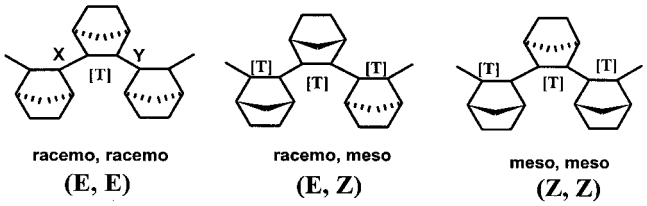

Scheme 3. Typical Configuration of Isotactic Polynorbornene

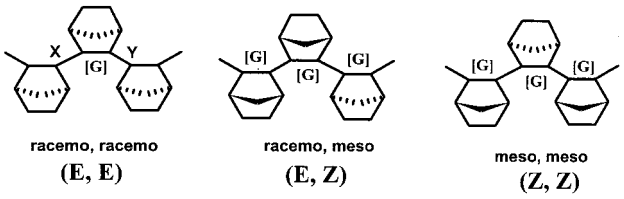

When including the C−C bond adjacent to the central norbornene unit, we have the following six basic conformations: T[T]T, T[G]T, T[T]G, T[G]G, G[T]G, and G[G]G. Here [X] = [G] or [T] has been determined during polymerization, as mentioned previously. For −N−N−N− and −N−N− sequences the conversion within the X[T]Y and the X[G]Y group experiences greater restriction than those in the isolated or alternating NB segments due to their less steric hindrance. The unaveraged conformation observed here would mostly be attributed to the NB dyad and triad sequence. Although the block is most possible in −N−N− dyad in reality, Schemes 2 and 3 illustrate with −N−N−N− triad sequence all possible conformations in syndiotactic and isotactic polynorbornene. In the syndiotactic case, it is impossible for norbornene to have all gauche configurations. Similarly, it is also impossible for the isotactic polynorbornene chain to bear consecutive trans configurations. The tacticity, meso (m) and racemo (r) with regards to the three-membered ring, is consistent with erythro (E) and threo (Z) nomenclature where three triad conformations, (E,E), (E,Z), and (Z,Z), are defined.

Despite its importance, little attention has been given to the conformational analysis of norbornene polymer and copolymers. Provasoli et al. have determined the conformer populations with the rotational-isomeric-state (RIS) approximation, where the distinct bond dihedral angles are determined by assuming nondistorted norbornene structure with molecular mechanics (MM3) minimization.[29] However, the study also found large conformation differences in the −N−N− or −N−N−N− sequence where strong effects arising from distortions of the norbornene rings superposed to the pure conformational effects. Because of this complexity, the ^{13}C NMR chemical shift calculation was not performed. A similar calculation also concluded that it is not possible to have chemical shift higher than 46 ppm for C2 and C3 carbons in all possible conformations in −N−E−N−E−, −E−N−E−, or −N−E−E− configurations.[30]

Scheme 4. Examples of Calculating the γ-Gauche Effect

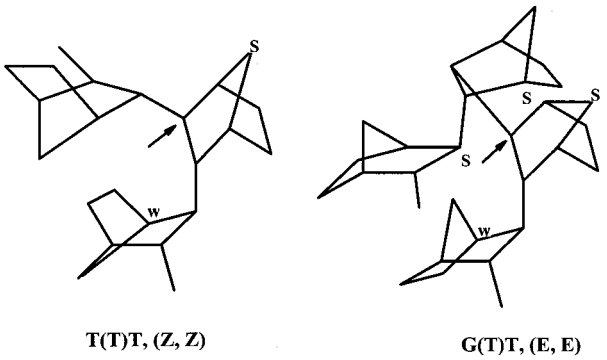

T(T)T, (Z, Z) G(T)T, (E, E)

Scheme 5. Conformation Interconversion of T(T)T to G(T)T

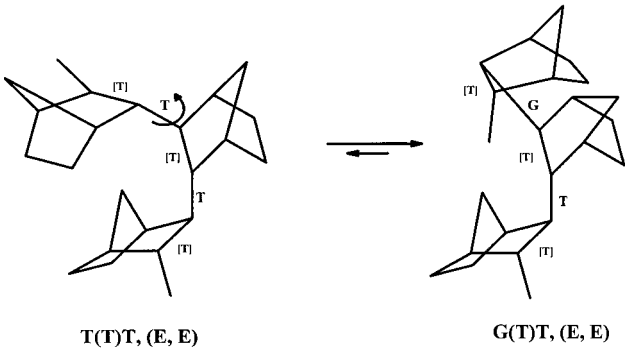

T(T)T, (E, E) G(T)T, (E, E)

Table 3. γ-Gauche Effect for All Syndio Configurations[a]

ring taticity	conformer	no. of γ-gauche effect (strong/weak)
(E, E)	T[T]T	2/1
(E, Z)		1/1
(Z, Z)		1/1
(E, E)	T[T]G	3/1
(E, Z)		3/1
(Z, Z)		3/1
(E, E)	G[T]G	2/1
(E, Z)		2/1
(Z, Z)		1/1
(E, E)	T[G]T	1/1
(E, Z)		2/1
(Z, Z)		1/1
(E, E)	T[G]G	1/1
(E, Z)		1/1
(Z, Z)		1/1
(E, E)	G[G]G	2/1
(E, Z)		2/1
(Z, Z)		2/1

[a] Iso configuration of norbornene is not favored (see text for details).

To make qualitative assignment of the shifts in PNB and COC with −N−N−N− and −N−N− blocks, simple counting of the γ-gauche effect [31,32] is performed, where we have assumed also the norbornene ring is not distorted. The shift calculations are demonstrated in two extreme cases shown in Scheme 4 for the norbornene CH carbons on the main chain (peak 1, designated by the arrow). The strongest γ-gauche effects are labeled as "s" and the weaker one by "w". The simple structure model also shows, except for the [G] configurations in NB units, that isotactic PNB experiences unusually high steric hindrance between the adjacent norbornene units (intrachain crowding and strenuous C−C single bond length). Although the catalyst rac-Et(Ind)$_2$ZrCl$_2$ bears a symmetry suitable for isotactic stereoregulation, a low amount of NB block with meso configuration is expected for this reason.

Table 3 lists the number of the γ-gauche effect calculated for all possible conformations with erythro-disyndiotactic and threodisyndiotactic triad conformers considered for the 18 possible conformers. The result shows the T[T]G conformer bears three strong and one weak γ-gauche effect while T[T]T and G[T]G conformers, two strong and one weak γ-gauche effects on the backbone carbon in norborene (peak 1). Similarly, the G[G]G conformer yields the greatest γ-gauche effects in the X[G]Y group. Although the final ^{13}C NMR shift value depends on the exact knowledge of the conformer potential energies, an estimation can still be made by recognizing that the X[G]Y conformer has a higher potential energy than the X[T]Y counterpart. This would lead to several resonances centered at two groups with a chemical shift separated slightly larger than one γ-gauche effect (∼2.8 ppm) on the order of 3−4 ppm. This result concurred with the ca. 2−4 ppm shift difference observed experimentally. The T[T]G group, with the strongest γ-gauche contribution, is reasonably assigned to the most upfield shift, while the 53 ppm peak is tentatively assigned to T[T]T and G[T]G groups of conformers. Other less populated conformers and possibly the isolated and alternating unit would locate between the two peaks.

Scheme 4 shows the NB rings experience severe crowding, and distortion in the three- and four-member rings on NB is necessary to accommodate neighboring NB units. However, the internal strain within norbornene is not likely to create a shift differences as high as 4 ppm, though it can modify slightly the calculated results. On the other hand, the tendency to release the internal strain served as the driving force for the conversion to a least restraint conformer, T[T]G.

Dual-component Gaussian decomposition (shown as the dashed curve) resolves the weight percentage of the two major groups of conformer being T[T]T + G[T]G = 55% and T[T]G = 45%. Similar calculation yields 40% and 60% for run 4 and 20% and 80% for run 3 respectively for T[T]T + G[T]G and T[T]G. A more quantitative calculation can be achieved with a suitable model developed to account for the NB ring internal strain, but for the present purpose, we retain the simplicity of the description to avoid a complicated situation.

For runs 1, 3, and 4, two groups of resonances are more clearly resolved with increasing fraction of block NB, where the NB block content is also high. However, in the case of low NB content (runs 5 and 6, [NB] < 45 mol %), where there are fewer NB block units, the downfield shoulder (at 53 ppm) becomes barely observable for runs 5 and 6. In alternating and isolated structures, cis-2,3-exo enchantment would be the major configuration as reported previously.[22,23b] However, such an enchantment does not predict any shift above 46 ppm, as mentioned previously.[30]

Scheme 5 shows one example of the one-bond conversion from T[T]T into the G[T]T conformer. In reality, cooperative conversion over several bonds occurs. These conversions are irreversible in the heat−melt cycle since the reverse process faces great resistance from increasing NB internal ring strain. The downfield portion in NMR does not recover either after quenching the annealed sample to liquid nitrogen temperature. In contrast with semicrystalline polymers where melt−

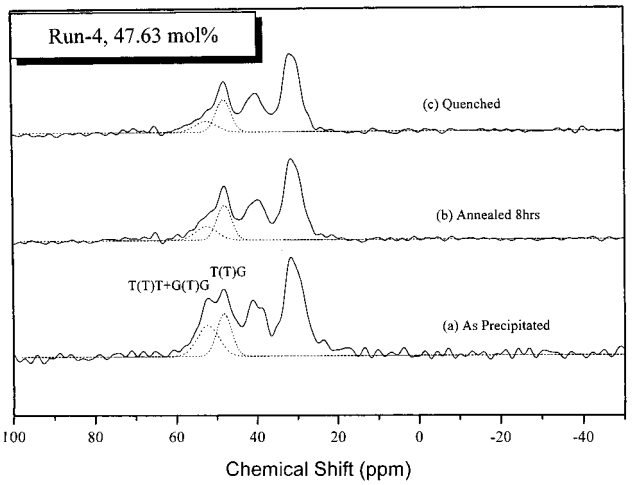

Figure 4. NMR CP/MAS spectrum of run 4 with different thermal treatments: (a) as precipitated, (b) annealed 8 h, and (c) quenched.

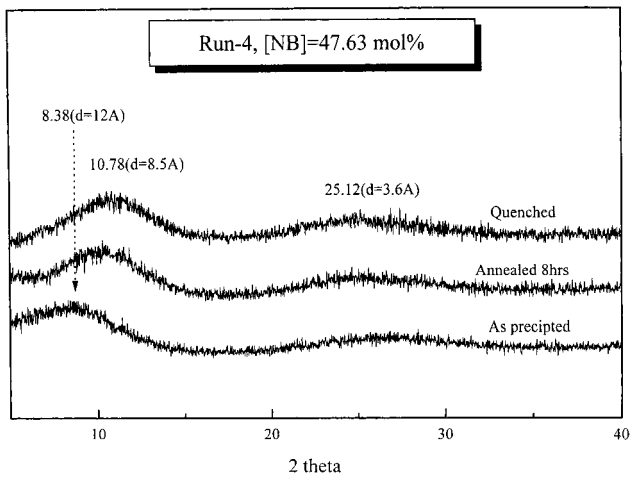

Figure 5. Synchrotron radiation powder X-ray diffraction of run 4 (a) before and (b) after extensive annealing.

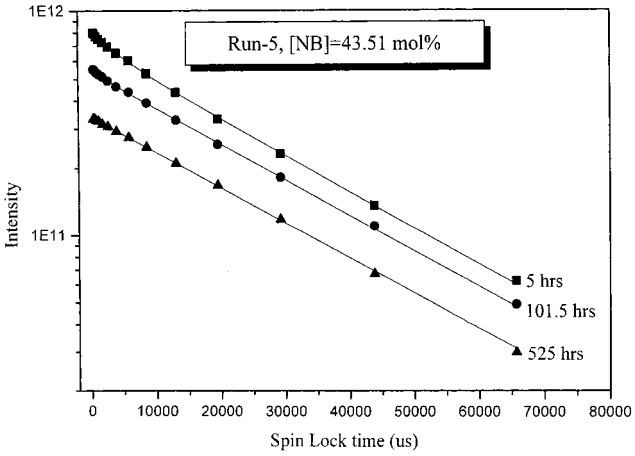

Figure 6. Semilog decay curve of COC $T_{1\rho}{}^{H}$ relaxation experiment with varying annealing time.

quench cycle retrieves the amorphous state, the stable conformation in COC appears frozen permanently once converted.

Run 3 (high NB content) and PNB (run 1) show similar conversion to the most thermodynamically stable T[T]G conformers with annealing. Nevertheless, complete removal of the T[T]T + G[T]G conformer is not possible, even after extensive annealing. It is plausible that a small amount of X[G]Y conformers or isolated and alternating NB has contributed to these absorptions. Recovery of the less stable conformer from quenching the extensively annealed sample is also not detected for these samples.

Densification. In the process of reaching the stable conformation, the persistent length increases and adjacent polymer fibular begin to self-assemble into short-range higher ordered arrangements. The net results of local packing are a decrease of the free volume with elevated T_g. Figure 4 shows the ^{13}C CP/MAS spectrum of run 4 at different stages of thermal treatments. When the original sample (Figure 4a) is annealed for 8 h, the downfield resonance of peak 1 (mainly T[T]T + G[T]G conformers, $\delta = \sim 53$ ppm) is substantially suppressed (Figure 4b) where the most thermodynamically stable conformation (T[T]G) was identified. Although there is no clear sign of conversion beyond this stage, the densification persists as the T_g continues to increase until annealing for 200 h (Figure 4c).

Previous wide-angle X-ray diffraction of poly(norbornene) homopolymer by Haselwander et al. found two diffraction peaks located at $2\theta = 10°$ and 19°.[20] The large angle scattering is assigned to the norbornene repeating unit, but the smaller diffraction with much larger d spacing remains unaccounted for. Later, a WAXD study of COC by MacKnight also revealed two halos which become more pronounced when NB content reaches 79 mol %.[21] The large scattering ($2\theta \sim 17°$) is assigned to the ethylene block and the norbornene alternating sequence, and the low angle peak ($2\theta \sim 11°$) has been assigned to the norbornene block unit since its intensity increases with increasing norbornene content. Closer examination of their results shows the low angle peak shift further to lower diffraction angles with increasing norbornene content. However, none of the studies reported scattering peak shifts with heat treatment. In the current study, X-ray diffraction (Figure 5), using run 4 as an example, also shows resolved double diffraction halos located at $2\theta = 20°$ and 11°. Here the norbornene content is lower than that in ref 21. The larger angle scattering ($d = 3.6$ Å) is attributed to the norbornene and ethylenes repeat unit length, which is consistent with all previous observations. However, the weaker halo at smaller scattering angle ($d = 12$ Å) sharpens and shifted to higher diffraction angle ($d = 8.5$ Å) with increasing degree of annealing. The present assignment explains the presence of the low angle peak in Haselwander's results, since there is no well-defined NB block length in PNB. It also accounts for the gradual lower angle shift with NB content reported by MacKnight since interchain spacing will increase with the presence of a more rigid NB block. Previous assignment of the low angle diffraction being attributed to NB block may be erroneous. The shift to higher angle with annealing readily evidenced that local chain packing in COCs occurred, and the peak sharpening indicated tighter distribution in the interchain spacing with greater ordering. For other COC samples with NB content below 47%, the low angle diffraction is less apparent, and the densification is harder to identify by this measurement. Nevertheless, densification is evidenced from the large T_g elevation for all COC samples.

The proton spin relaxation time in the rotating frame, $T_{1\rho}{}^{H}$, provides the information regarding the change of dynamics during densification. Based on a crude estimation of proton spin diffusion, this measurement is

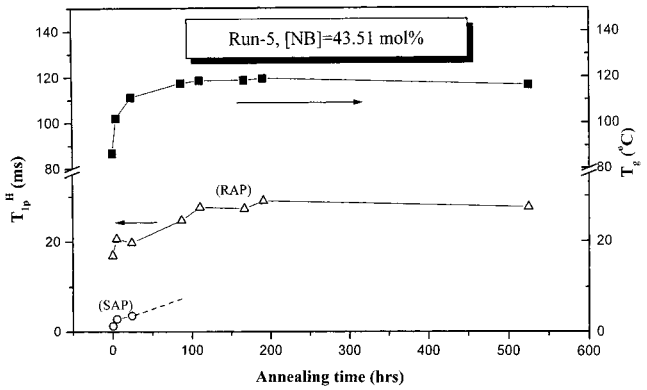

Figure 7. T_g (top trace) and $T_{1\rho}^H$ (lower trace) changes with annealing time for run 5.

subjected to a limited domain resolution of ~50 Å. Figure 6 shows the variation of $T_{1\rho}^H$ relaxation time for the COC (run 5) with annealing where the decay is taken from the integrated intensity of signals occurring between 28 and 32 ppm (ethylene CH_2 and norbornene CH_2 resonances). Two $T_{1\rho}^H$ exponential decays are apparent at the initial stage of annealing, which gradually coalesce to a single relaxation after annealing. In contrast, DSC shows only single T_g throughout all stages of annealing for all samples. Figure 7 summarized the changes of both $T_{1\rho}^H$ and T_g (run 5) with annealing. The two dynamic heterogeneous domains identified by $T_{1\rho}^H$ should therefore be smaller than can be differentiated by T_g. The coalescence of relaxation after extended annealing suggested that homogenization in either the composition or the mobility has occurred. Most interestingly, the time where the two relaxation values coalescence coincide with the instant when conformation conversion ceases. Other COC samples (runs 1, 3, and 4) also indicated coalesces of dual relaxation after extended annealing. These observations are not consistent with the possibility of the presence of separated PE-rich and PNB-rich domains (with size larger than 50 Å). Besides, PE crystallization is not found for those samples. The two $T_{1\rho}^H$'s are more reasonably attributed to domains with different mobility, carrying similar chemical composition. Knowing that the short $T_{1\rho}^H$ originates from more mobile COC, the result provide the microscopic understanding that extended annealing (run 5, roughly 60% of the mobile fraction and 40% of the rigid fraction) has homogenized chain mobility which led to greater overall rigidity with longer averaged $T_{1\rho}^H$. This understanding is consistent with the picture that conformation conversion has converted the relatively softer domain to more rigid domain segment and led to the increase of the hard domain fraction. The detailed morphology of microdomain phase separation on the order smaller than 50 Å would be the subject of a separate study using small-angle neutron scattering techniques.

Figure 8 summarizes with run 4 of the T_g elevation and the change of conformation from ^{13}C NMR spectra during different stages of annealing. The result suggested that the initial rapid rise of T_g originated from the conformation conversion, which produced longer rigid length with lower entropy in the amorphous polymer, and the subsequent T_g increase corresponds to the densification with more ordered local packing. This phenomenon has not been reported in previous COC studies, possibly due to an insufficient amount of long NB block unit as it is in the current samples, or the densification has already been reached with prior heat treatments.

Since all trans or T[T]G[G] chain conformations in COC are not energetically favored (vide supra), crystallization of COC is extremely difficult even in the highly stereoregulated case. This argument is further supported by the understanding that periodical T[T]G[G] or all T[T]T[T] conformations in COC, required for crystallization, is difficult if not impossible to reach.

The few characteristics associated with the local packing in COC (poly(norbornene-*co*-ethylene) are sum-

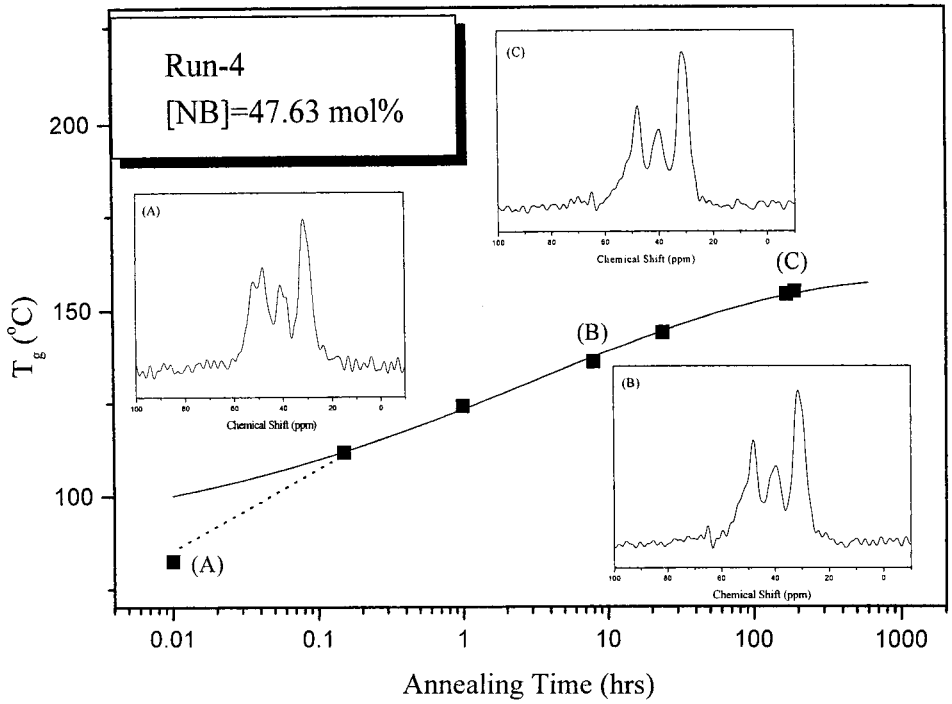

Figure 8. T_g elevation and the ^{13}C NMR spectra during each stage of the annealing for run 4 illustrate the relationships between conformation conversion and formation of rigid amorphous phase.

marized: (i) phenomenal glass temperature variations, (ii) dense packing, (iii) conformation ordering, (iv) smaller distribution in interchain spacing, and (v) reduction of the nearest-neighbor COC chain spacing to 8.5 Å. Previously, the dense packing in glassy bisphenol A polycarbonate shows similar chain orientational order and has been described by the bundle model where the carbonyl carbon to quarternary carbon in the nearest-neighbor interchain distance is shortened to about 6 Å.[11] For polycarbonate-like polymer, the π-flip gate from synchronization of the arrival of a lattice phonon leads to the reduction in intermolecular steric barrier. However, for COC the densification continues after the stable conformation is reached, and there is no apparent π-flip mechanism available in COC. Furthermore, there are no specific interchain interactions, apart from the fundamental London dispersion force, to adhere the bundle. The possible densification mechanism in COC may involve that proximal NB unit stiffens the chain first by the converted conformation, which reduced the entropy of the nearby fibular rigid segment. The reduction of interchain barrier which leads to the later stage of local packing in COC is not consistent with the cooperative motion given by the bundle model.[16] Instead, it is more likely due to random sources achieved through chain diffusion.[15] As far as the kinetics is concerned, the later process would be much slower in comparison.

Conclusions

Cyclic olefin copolymer (COC), made by ethylene and norbornene catalyzed by *ansa*-ethylene bis(indenyl) zirconium dichloride (Et[Ind]$_2$ZrCl$_2$)/methyl aluminoxane (MAO), shows higher concentration of norbornene block (−N−N−N− and −N−N−). Annealing has raised the T_g of the nominally amorphous PNB and COC's to nearly 120 and 30−80 °C, respectively. The study shows these COC exhibited conformation conversion which increases the persistent length and facilitated local packing into more ordered morphology. Unlike most amorphous polymers, where conformers are freely converted via rapidly chain orientation, norbornene chain reorientation is highly restricted. Failure to sample all conformations within the NMR time scale produced two resolved groups of resonances at 53 and 49 ppm in the ^{13}C spectrum of the CH carbon in the norbornene unit which are assigned to T[T]T + G[T]G and T[T]G conformers after counting all possible γ-gauche effects. Two separate relaxations coalesce to a longer relaxation component with progressive annealing in $T_{1\rho}{}^{H}$ measurements, suggesting that the local packing has averaged the chain mobility leading to single and more rigid overall structure. The low angle diffraction halos in synchrotron source X-ray data provide direct identification that a contraction in the averaged spacing is reduced from ca. 12 to 8.5 Å, and the distribution of the interchain spacing becomes tighter upon extensive annealing.

Acknowledgment. Financial support of this research is provided by the National Science Council of Republic of China under Contract NSC-88-2113-M-008-004.

References and Notes

(1) Benedikt, G. M.; Goodall, B. L.; Marchant, N. S.; Rhodes, L. F. *New J. Chem.* **1994**, *18*, 105.
(2) Kaminsky, W.; Bark, A.; Arndt, M. *Macromol. Chem. Macromol. Symp.* **1991**, *47*, 83.
(3) Kaminsky, W.; Bark, A. *Polym. Int.* **1992**, *28*, 251.
(4) Herfert, N.; Montag, P.; Fink, G. *Makromol. Chem.* **1993**, *194*, 3167.
(5) Kaminsky, W. *Macromol. Chem. Phys.* **1996**, *197*, 3907.
(6) Guerra, G.; Vitaliano, V. M.; Rosa, C. D.; Petraccone, V.; Corradini, P. *Macromolecules* **1990**, *23*, 1539.
(7) Kaminsky, W.; Arndt, M.; Bark, A. *Polym. Prepr.* **1991**, *32*, 467.
(8) Kaminsky, W.; Engehausen, R.; Kopf, J. *Angew. Chem., Int. Ed. Engl.* **1995**, *34*, 2273.
(9) Ruchatz, D.; Fink, G. *Macromolecules* **1998**, *31*, 4674.
(10) Chu, P. P.; Huang, W.-J.; Chang, F.-C. *Polymer* **2000**, *41*, 401.
(11) Klug, C. A.; Zhu, W.; Tasaki, K.; Schaeler, J. *Macromolecules* **1997**, *30*, 1734.
(12) Cheng, S. Z. D.; Wu, Z. Q.; Wunderlich, B. *Macromolecules* **1987**, *20*, 2802.
(13) Tritto, I.; Boggioni, L.; Sacchi, M. C.; Locatelli, P.; Ferro, D. R.; Provasoli, A. *Macromol. Rapid Commun.* **1999,** *20*, 279.
(14) Lasarov, H.; Pakkanen, T. T. *Macromol. Rapid Commun.* **1999**, *20*, 356.
(15) Hutnik, M.; Gentile, F. T.; Ludovice, P. J.; Suter, U. W.; Argon, A. S. *Macromolecules* **1991**, *24*, 5962.
(16) Whitney, D.; Yaris, R. *Macromolecules* **1997**, *30*, 1741.
(17) Goeta, J. M.; Wu, J.; Yee, A. F.; Schaefer, J. *Macromolecules* **1998**, *31*, 3016.
(18) Huang, W. J.; Chang, F.-C.; Chu, P. P. *J. Polym. Res.* **2000**, *7*, 51.
(19) Ruchatz, D.; Fink, G. *Macromolecules* **1998**, *31*, 4669.
(20) Haselwander, T. F. A.; Heitz, W.; Krugel, S. A.; Wendroff, J. H. *Macromol. Chem. Phys.* **1996**, *97*, 3435.
(21) Rische, T.; Waddon, A. J.; Dickinson, L. C.; Macknight, W. J. *Macromolecules* **1998,** *31*, 1871.
(22) Ruchatz, D.; Fink, G. *Macromolecules* **1998,** 31, 4681.
(23) Cherdron, H.; Brekner, M.-J.; Osan, F. *Angew. Makromol. Chem.* **1994**, *223*, 121.
(24) Bergstrom, C. H.; Vaananen, T. L. J.; Seppala, J. V. *J. Appl. Polym. Sci.* **1997**, *63*, 1071.
(25) (a) Bergstrom, C. H.; Starck, P. G.; Seppala, J. V. *J. Appl. Polym. Sci.* **1998**, *67*, 385. (b) Bergstrom, C. H.; Vaananen, T. L J.; Seppala, J. V. *J. Polym. Sci., Part A: Polym. Chem.* **1998**, *36*, 1633. (c) Bergstrom, C. H.; Seppala, J. V. *J. Appl. Polym. Sci.* **1997**, *63*, 1063.
(26) Gomez, M. A.; Tonelli, A. E. *Macromolecules* **1991**, *24*, 3533.
(27) Huang, J.-M.; Chu, P. P.; Chang, F.-C. *Polymer* **2000**, *41*, 1741.
(28) Sticky speaking, there is no well-defined trans or gauche conformation for the NB single bond on the main chain. The [T] or [G] symbols are used here for convenience to differentiate the possible geometries in NB as defined in Scheme 1. This conformation for the single bonds adjacent to NB follows the conventional definition.
(29) Provasoli, A.; Ferro, D. R. *Macromolecules* **1997**, *10*, 874.
(30) Provasoli, A.; Ferro, D. R.; Tritto, I.; Boggioni, L. *Macromolecules* **1999**, *32*, 6697.
(31) (a) Gomez, M. A.; Jasse, B.; Cozine, M. H.; Tonelli, A. E. *J. Am. Chem. Soc.* **1990**, *112*, 5881. (b) Elias, H.-G. *Macromolecules*; Plenum Press: New York, 1983.
(32) Tonelli, A. E. *NMR Spectroscopy and Polymer Microstructure*; VCH: New York, 1989.

MA000494K